Proceedings World Geothermal Congress 2010
Bali, Indonesia, 25-29 April 2010

Seismic Tomography and Long-Period Earthquakes Observation and Modelling at the Hengill Geothermal Volcanic Complex, Iceland

Philippe Jousset[1], Christian Haberland[2], Klaus Bauer[2], Knutur Arnason[3], Michael Weber[2], Hubert Fabriol[1]

1: BRGM Orléans, France; 2: GFZ Potsdam, Germany; 3: ISOR, Iceland

Corresponding author: p.jousset@brgm.fr

Keywords: Broadband seismology, geothermal energy, tomography, structure, exploitation, long-period earthquakes.

ABSTRACT

Hengill volcanic complex is located at a triple-junction between two segments of the spreading ridge between North American plate and European plate, and a transform fault (South Iceland Seismic Zone). This area is subject to intense seismic activity, which is monitored continuously by a permanent seismological network, the SIL network of the Icelandic Meteorological Office. A well-developed geothermal system is exploited and the extracted vapour allows Icelanders to sustain for part of their needs in power supply and heat. In order to improve the understanding of the relationships between the seismic activity and geothermal exploitation, a network including 7 broadband seismological stations was set up from June 26th, 2006 until October 17th, 2006, in the framework of the FP6 funded I-GET project. Data analysis allowed us to detect more than 600 earthquakes, amongst which long-period (LP) earthquakes were observed. We locate 339 micro-earthquakes with clear P- and S- arrival times and we improve the knowledge of the velocity structure by performing a joint inversion of hypocenters and 3D tomography. We find a high velocity anomaly in the area of Olkelduhàls at about 2-4 km depth and a low v_P/v_S ratio anomaly beneath the northern part of Mt. Hengill below 4-5 km. The northern and western limit of the detected anomalies but cannot be determined accurately by lack of coverage of the network in those areas. We compare our velocity model and resistivity anomalies obtained from electrical and TDEM surveys. The new structural features at Hengill suggest new opportunities for studying the relation between local seismicity and fluid exploitation. We find that LP observed earthquakes happen close to exploitation wells when extraction rate is changed. We model LP earthquakes using a wave propagation modelling finite difference scheme with topography, velocity model and attenuation. We find that the synthetic LP earthquake has frequencies similar to those recorded in the observed LP earthquakes. This suggests that the resonance of a part of the geothermal system may explain characteristics of low-frequencies and that a sudden change of pressure due to exploitation rate change may be the trigger for LP seismicity.

1. INTRODUCTION

The objective of seismology in geothermal areas is to contribute to the imaging and monitoring of hydrothermal systems. We want to image the extension of the geothermal system to possibly locate the productive fractures, and to follow with time the evolution of the geothermal resource. The analysis of the natural and induced seismicity is usually performed with "short-period" seismometers data (frequency band >1 Hz) (e.g., Fabriol et Beauce, 1997). Analysed signals correspond to micro earthquakes linked to rock rupture that generate high seismic frequencies, and associated with stress changes due to fluid displacement or cooling. These analyses allow determining hydro mechanical properties (e.g., permeability) of geothermal systems (Audigane, 2000), or fracture orientation (Evans et al., 1996).

The analysis of seismic broadband signals (0.01 Hz to 100 Hz) allows accessing to structural and dynamical parameters on active volcanoes. For instance, the volcanic conduit at Stromboli volcano, Italy, was imaged from the analysis of Long Period signals (0.2 – 5 Hz) and tremor (Chouet et al., 2003). Such LP signals with similar duration and frequency content characteristics were reported on volcanoes (e.g., Chouet, 1996), oil fields (e.g., Dangel et al., 2003) and geothermal fields (e.g., Jousset, 2006). Chouet (1986) proposed a model that explains the spectral content and the duration of long-period events: on the basis of the results of Biot (1952) and of Aki et al., (1977), he developed a fracture model in which the mechanical interaction between the fluid within the fracture embedded in the elastic solid is considered as a coupled system and analysed completely: the fluid-filled fracture resonates following several modes. The resonance is described analytically by Ferrazini et Aki (1987). The fundamental mode, very energetic, comprises "slow waves", also called "crack-waves", which travel along solid/fluid interfaces (Jousset et al., 2003). The "slow wave" frequency content is dependent on the geometrical and physical properties of the fluid, of the fracture and of the hosting rock. The detailed spectral analysis of LP earthquakes at volcanoes allowed many studies to improve our understanding of structural and dynamical features of volcanic and hydrothermal systems (e.g., Kawakatsu et al., 2000; Almendros et al., 2001; Nakano et al., 2003; Chouet et al., 2003; Kumagai et al., 1999; 2002).

We describe in Section 2 our general approach to study geothermal fields with broadband seismology. In section 3, we present data acquisition at Hengill geothermal field, Iceland. In section 4, we analyse the structure of Hengill geothermal field by showing results of the seismic tomography performed using VT earthquakes. In section 5, we focus on the analysis of long-period earthquakes observed during our experiment.

2. BROADBAND SEISMOLOGY AS A TOOL TO IMAGE AND MONITOR GEOTHERMAL FIELDS

Under the hypothesis that the physical mechanisms generating LP earthquakes and the resonance within volcanic and exploited geothermal systems are the same, broadband seismological networks are able to give insights for exploration and monitoring of exploited geothermal systems. In order to assess the source mechanisms of LP earthquakes, reflecting the mechanical behaviour of rocks

under fluid pressure, lower frequencies need to be recorded, e.g., using broadband seismometers (Jousset et al., 2004b).

Three themes may be developed from the analysis of the broadband signals (Figure 1): 1) Structure: earthquakes location, waveform and spectral analysis, tomograph 2) Dynamics: fluid movement, hydraulic fracturing, physical properties of the media, .3) Seismic hazard knowledge.

Within this strategy, wave form inversion has been shown to be very useful to infer source mechanism of LP earthquakes (Legrand et al., 2000 ; Chouet, 2006). In order to perform the waveform inversion, we need 3 fundamental information 1) Seismological observations from a network of seismic stations; those observations need to be calibrated and having a frequency band adapted to the frequency of the searched signals; 2) A collection of Green's functions, i.e., synthetic seismic signals, computed from the modelling of the wave propagation in 3D in complex media (solid, liquid and gas) at high temperature. 3) An algorithm for inverting data, which looks for the selection of Green's functions within the whole collection, that best fit observations in the least square sense. The result is a hypocenter location and the moment tensor of the source and therefore the source mechanism.

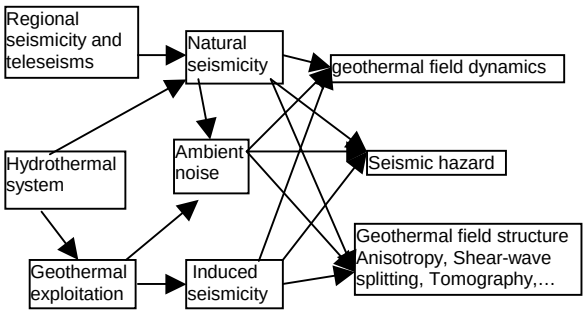

Figure 1 – Strategy for the study of geothermal systems using broadband seismology.

Therefore, the analysis of the signals recorded by a network of broadband seismometers allows direct observation of interactions between fluids and solid (e.g., in fractures), where those fluids sustain sudden pressure variations. We applied this approach at the Hengill geothermal system, by setting up a seismological network comprising 7 broadband seismometers. We processed data using classical techniques of seismic analysis, and we modelled seismic waves using a finite difference code (Jousset et al., 2004a), recently transformed in 3D.

3. DATA ACQUISITION

3.1 Geological Setting

The Hengill geothermal area is about 200 km^2 (Arnorsson et al., 2008). It is a volcanic complex located in the southern end of the western volcanic zone (WVZ) of Iceland. It is at the junction of the WVZ, the Reykjanes Peninsula (RP), which is the landward extension of the Reykjanes spreading ridge, and the South Iceland Seismic Zone (SISZ), which is a transform zone, transferring a part of the crustal spreading from the WVZ to the eastern volcanic zone (Einarsson, 2008). The Hengill volcanic complex hosts three main volcanic centres, which are, listed from SE to NW and decreasing age, Grændalur (0.3-0.5 My), Hrómundartindur on the decline and Hengill at the peak of activity. The Grændalur volcano was substantially eroded during glacial time, but Hrómundartindur and Hengill consist mainly of little eroded hyaloclastite. Both Hrómundartindur and Hengill have erupted in postglacial times. Hrómundartindur last erupted about 11 thousand years ago and Hengill 5 thousand and 2 thousand years ago. The extrusive volcanic products are mainly basalts but with significant occurrences of acidic rocks SW of Mount Hengill Sigmarsson et al., 2008). The Grændalur-Hrómundartindur part of the Hengill volcanic complex is seismically very active (Jakobsdottir, 2008). The Hengill central volcano is bisected by about 3-5 km wide and about 40 km long fissure swarm, extending N30°E, from the coast and to the NE towards lake Þingvallavatn. The fissure swarm was active in 1789, with extensive rifting and subsidence. The Seismic Iceland Lowland (SIL) network (Stefansson et al., 1993) is a permanent seismic network operated by the Icelandic Meteorological Office. In the period from 1991 to 2001 high seismic activity occurred in the eastern Hengill area but with different tectonics. The SIL network recorded over 90 thousand earthquakes. Similar active periods occurred around 1915 and 1950-1955.

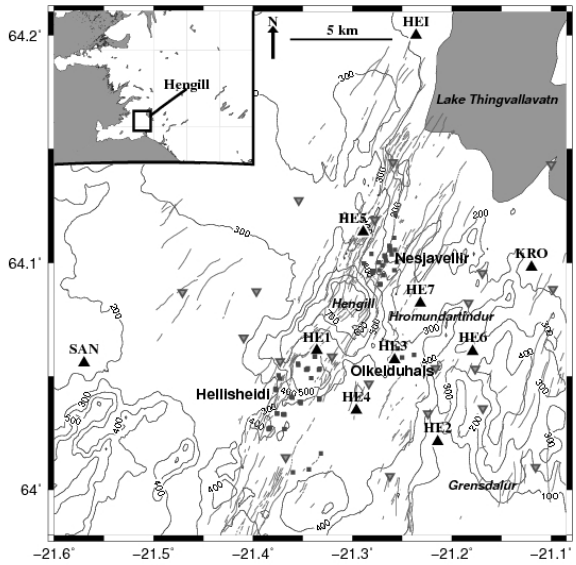

Figure 2 – Topographic map of Hengill Volcano, Iceland, with the location of the broadband seismological stations (HE1, HE2, HE3, HE4, HE5, HE6, HE7) and SIL network stations (KRO, SAN, HEI). Small gray squares are locations of geothermal wells; they are grouped in three areas (Nesjavellir, Hellisheidi and Olkelduhàls). The three main volcanic centers are indicated in italics (Hengill, Hromundatindur and Grændalur). Grey lines represent fissure swarms at surface. Inlet shows the location of Hengill volcano in Iceland.

3.2 Data Acquisition

We set up a network of 7 broadband stations (Güralp CMG-40TD and CMG-3ESPD, recording at a sampling rate of 100 Hz) from the 19th of June until the 20th of October 2006 (Jousset and François, 2006). Data from our network was augmented with data from 3 stations from the SIL network (Jacobsdottir, 2008), set up to record data continuously (Figure 2).

3.3 Data Processing

Our data set comprises three sorts of files that had to be arranged in a common format for consistent processing. Reading, processing and classifying seismic data have been

performed with an integrated tool, called Seismotool (Jousset, 2006) written in Matlab. It is an interactive platform in which automatic detection and processing was applied to the 4 months data set using sliding windows, as if data would be acquired in real-time. Several tasks are automatically performed: 1) read data files according to the file format at all stations for a duration of 3 hours; 2) perform event detection using a STA/LTA technique on the envelope of the signals; 3) perform event calibration according to the instrumental response provided by the constructor and stored in a database; 4) classify events according to the number of stations at which the detection flag was raised, and 5) build a list of detected and classified events, i.e., an earthquake catalogue.

4. JOINT INVERSION OF HYPOCENTER LOCATION AND 3-D VELOCITY MODEL

To improve our knowledge of the 3-D structure of exploited geothermal systems, we perform local seismic tomography inversions, with micro-earthquakes recorded by seismic network. Previous tomography studies at Hengill area (e.g., Miller et al., 1998) reveal the main structural features of the volcanic area and the triple junction, but they are not sufficiently detailed for a accurate analysis of the structural features of the geothermal system itself. In particular, the v_P/v_S ratio and attenuation measurements are very diagnostic of pore-fluid and temperature conditions when used in conjunction with v_P (Evans et al., 1994). In addition, the improvement of the velocity model is required in order to locate long-period earthquakes (e.g., Lokmer et al., 2007).

Data required to perform 3D seismic tomography are P-wave and S-wave time arrivals. In order to pick the compressional (P) and shear (S) arrival times required for the tomography from the VT earthquakes, we implemented in Seismotool (Jousset, 2006) an algorithm consisting in computing An Information Criteria (Akaike, 1973) directly on the amplitude vector of the seismogram (Maeda, 1985). For a digital seismogram x[1,N] of length N samples, the AIC value is defined as:

$$AIC(k)=k \log\{var[x(1,k)]\} + (N-k-1) \log\{var[x(k+1,N)]\} \quad (1)$$

where k ranges through all the seismogram samples, var means the variance and log is the logarithm.

Our picking method minimizes errors due to change of operator. Error estimation on picking is also implemented in Seismotool. The error is estimated by the use of two picking values instead of only one as usually done. The two picked times define a time interval during which the wave arrival time might be located with uniform probability.

We invert 339 micro-earthquakes with clear P- and S-arrival times detected by at least 4 stations (2266 P- and 2432 S- waves arrival times) to apply tomography inversion of the compression P-wave and shear S-wave structure of the geothermal reservoir. We use the computer program SIMULPS12 (Evans et al., 1994), which solves simultaneously for earthquake locations and crustal structure by the iterative damped-least-square method. The program VELEST (Kissling, 1994) provides one-dimensional v_P (and v_S) models used as a starting point for the inversion. A careful choice on the earthquakes and inversion parameters has been done prior to the inversion (Eberhart-Phillips, 1993).

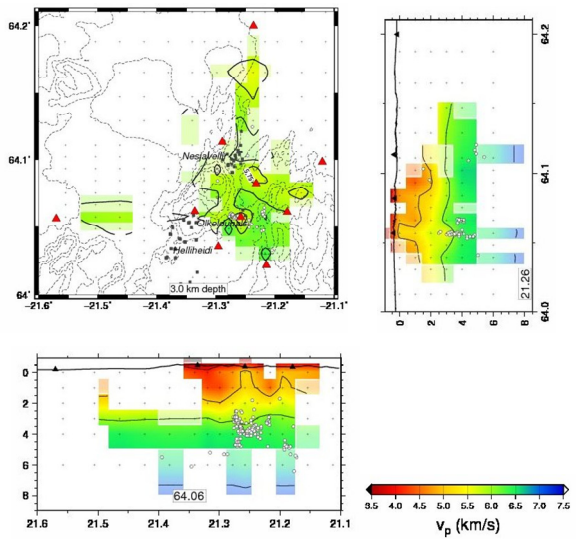

Figure 3 – Vp velocity model from the joint inversion of hypocenters and velocity model for two vertical slices and an horizontal slice at 3 km depth.

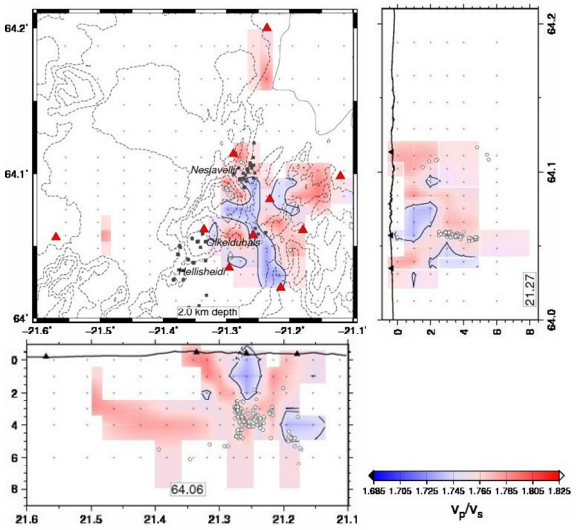

Figure 4 – Vp/Vs ratio from the joint inversion of hypocenters and velocity model at 3 km depth.

The structure is parameterised by the values of the P-wave velocity v_P and the v_P/v_S ratio at the nodes of a 3-D grid, and the observed P- and S- arrival times are inverted by an iterative least-squares method to determine simultaneously the coordinates of earthquakes hypocenters and the values of v_P and v_P/v_S ratio at the grid nodes. The solution is obtained by iterative damped least squares inversion. The full resolution matrix is calculated (Yao et al., 1999). Prior to each 3-D inversion, the damping parameter is chosen empirically by evaluating a trade-off curve of data variance and solution variance as the damping varies with the model grid and the data set (Haberland et al., 2006). We performed a series of simultaneous hypocenter-velocity inversions progressively increasing the complexity in the model and refining the mesh of the 3-D grid. Data variance decreased after each step. We started using a coarse 3-D grid spacing of 2 km, with several nodes outside the target geothermal system, in order to constrain the volume that our data set can image. Then we inverted our data set with a denser grid down to a grid spacing of 1 km (Figure 3). The same approach has been used to compute the v_P/v_S ratio (Figure 4).

The joint inversion successfully confirmed the known structural features and provided a increased resolution. In order to validate our result, a series of tests were performed including a checkerboard test and rays tracing, which reveals that our data set and network covers well the area of interest (Jousset et al., in press).

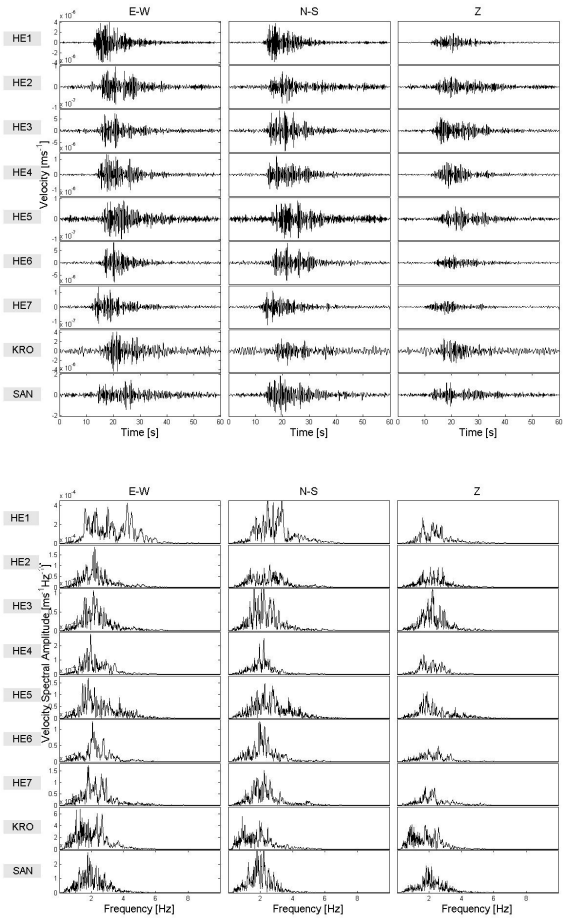

Figure 5 - Long-period earthquake on 1st July 2006 at Hengill. (top) 60 seconds of unfiltered signal (bottom) frequency spectra. Note that the frequency content at all stations is similar. We believe it is a source effect rather than a path effect.

5. ANALYSIS AND MODELLING OF LONG-PERIOD EARTHQUAKES

Non-double earthquakes were recorded at Hengill (Julian et al., 1997) and were associated to fluid migration in the geothermal system. Amongst the earthquakes recorded at Hengill from the 19th of June until the 20th of October 2006, 20 events have characteristics of Long-Period earthquakes, i.e., their durations last several tenths of seconds and their frequency content reveals peaks of resonance between 0.2 to 5 Hz (Figure 5).

In order to model LP earthquakes at Hengill, we assume that the geothermal reservoir may be simplified as a "container" in which the fluid content is much higher than elsewhere in the surrounding crust. Such model is consistent with observations revealing that fracture porosity is usually higher inside a geothermal reservoir; it is also usually a small fraction of matrix porosity (Gruszkiewicz et al., 2001). Matrix porosity may be higher or lower inside a system. In addition, as pressure drops after production begins, geothermal fields often begin to boil and develop a steam cap (e.g. Allis, 2000). Therefore, except near injection wells, a produced geothermal field usually has lower fluid pressure (e.g., Allis and Shook, 1999) and some parts may have lower water saturation in comparison to the surrounding rock (e.g., Hsieh and Ramey, 1978).

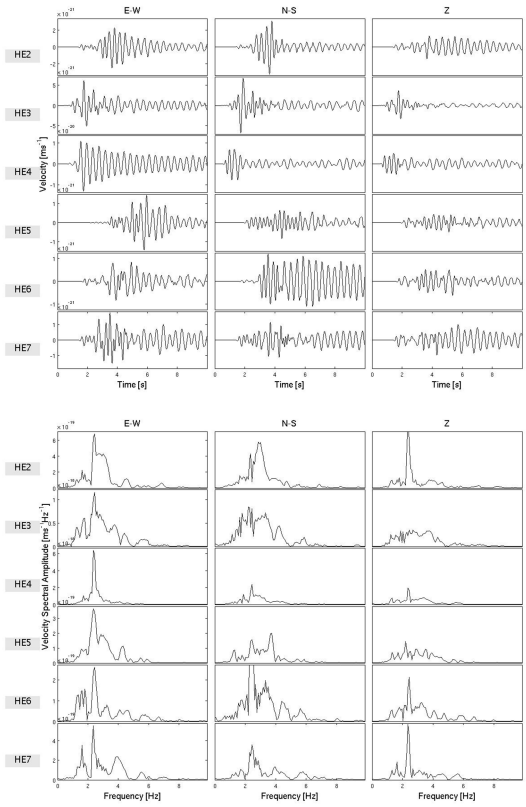

Figure 6 – Synthetic long-period earthquake modeled using 3D finite-difference including velocity model and topography of Hengill. No attenuation is included in this case. The grid spacing is 100 m in horizontal direction and 50 m in vertical direction. Time step is 0.003 s. (top) 10 s of unfiltered signal (bottom) frequency spectra.

The very high compressibility of the steam cap dampens pressure transients in the permeable system, but it also increases the impedance contrast between the interior of the geothermal system and its surrounding. Stresses are perturbed by localized chilling due to injection and, over a longer term, by deformation along the margins and interior of the volume that compacts as pressure and temperature drops. Several geothermal fields show a seismic response to sudden large changes in field production, suggesting that even heavily damped pressure transients can trigger micro earthquakes (e.g., Romero et al., 1994). Note that at Hengill the injection wells are located outside the aperture of our network. The observed LP earthquakes are not related to any fluid re-injection but to extraction flow only.

In our model, the fluid container may be such an area where crack and fracture density is higher, e.g., due to higher porosity, and from which geothermal fluids are extracted. This area may be as small as a crack, or be larger as the whole geothermal reservoir. Seismic velocities and densities are therefore different than in the surrounding rocks, but may well not be resolved with seismic tomography. When a sudden change of fluid pressure (either due to natural earthquakes or due to a change in the extraction rate) occurs within or in the vicinity of the fluid container, seismic waves are generated and are trapped in

this area of high fluid content, due to large impedance contrast between the fluid properties inside the container and surroundings rocks. The frequency content of the seismic signals is directly related to the size of the container and the physical properties of the rock and fluid, through the stiffness factor (Ferrazzini and Aki, 1977).

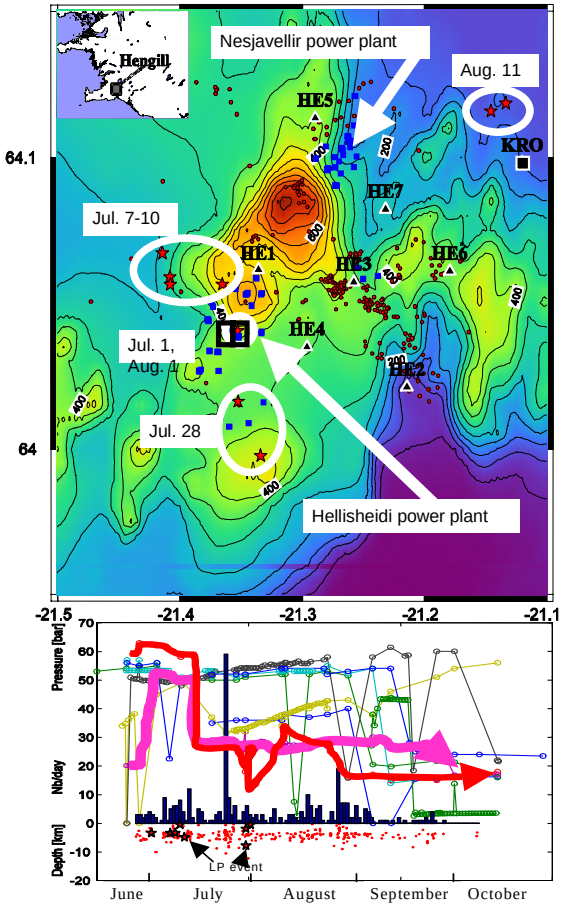

Figure 7 – Relation between seismicity and geothermal fluid production at various wells at Hengill. (Top) Seismicity at Hengill. Black triangles: broadband stations; black squares: SIL stations. Red circle: epicentres of VT earthquakes. Red stars: epicentres of LP earthquakes. White ellipses underline the time clusters of LP earthquakes. Blue squares: exploitation wells. Black squares: location of wells where head pressure of well is highlighted. (Bellow) Time evolution of VT earthquakes (red circles) and LP earthquakes (stars) depths; daily instances of VT earthquakes; pressure at various wells. Red and pink curves represent the pressure evolution for wells located at the black rectangles in the map (see top).

We implement this model within a 3D finite-difference code (Jousset et al., 2004) for modelling synthetic LP signals. Topography, 1D velocity model and attenuation of waves are also implemented. The computational grid covers the central area of our network (12*12*7 km).

This modelling approach allows us to test various source mechanisms and fluid container geometry and physical properties by analysing the frequency content of the synthetics as a function of the model parameters. For example, Figure 6 shows 10 s of synthetic signals for a resonance parallelepiped located at 2 km depth to the East of Hellisheidi power plant (see location in Figure 2). This 500*100*600 m^3 container is filled with a fluid with P-wave velocity Vp=1700 ms^{-1}; S-wave velocity Vs=0 ms^{-1} and density of 1200 $kg.m^{-3}$. Note that the frequency content at all stations is similar, and similar to the frequency content of the observed signals.

Observed LP earthquakes seem to occur close to exploitation wells, when production rate changes. The occurrence of LP events seems to be correlated to pressure changes at wells. However, it is difficult to conclude definitively on their origin, as most of them are located outside the aperture of the network. As the signal is emergent, it is difficult to obtain an accurate location from accurate P-wave picking. Other techniques like amplitude locations or waveform inversion may help in discriminating between possible source mechanisms.

6. CONCLUSIONS

The velocity structure of the Hengill area, as revealed by the joint 3D tomography inversion, was compared to other geophysical data. The location of high P-wave velocity coincides with area where a deep conductor is at shallowest depth (about 2-3 km), according to the results from the 1D inversion of TEM and MT soundings and 3D inversion of MT soundings acquired within the I-GET project (Arnasson et al., 2009; Figure 8). No sign of attenuation of seismic S-waves is observed under the Hengill area, indicating absence of extensive magma chambers at depth. The area where high velocity bodies are found correlates with positive Bouguer anomalies, indicating dense rocks at depth.

The seismicity is located at the top boundary of the high velocity body at the SE of Mount Hengill. This area corresponds to the NW-SE oriented low resistivity anomaly at the depth of 3-5 km. The intense seismic activity from 1991 to 2001 revealed a distinct transform tectonics. The anomaly is under an area where E-W oriented faults meet N-S oriented faults. Synthetic Aperture Radar Interferograms (InSAR) show that between 1993 and 1998 there was a considerable uplift going on (up to about 18 mm/year) with the centre of the uplift SE of Mount Hengill. All the different data sets can be explained by hot but mostly solidified intrusions and dikes. The accumulation of intrusions is facilitated by the transform tectonics. The recent intense seismic activity and uplift are thought to reflect an intrusion phase. The reason why the intrusion/dike complex is so highly conductive is not well understood. It can, however, be concluded with relatively good confidence that the deep conductors reflect very hot rocks that are heat sources for the geothermal systems in the Hengill area.

During our experiment, the recorded micro-seismic activity is probably related to the cooling of deep magmatic bodies and to geothermal fluids activity within Hengill volcanic complex.

We found evidence that the geothermal system exploitation may trigger long-period earthquakes. They may be related to the change of pressure at the vicinity of the wells due to variable exploitation rate of geothermal fluid. We modelled the LP earthquake as the resonance of a fluid container, which are excited by sudden pressure variation in association with the fluid extraction rate fluctuation. Further investigations are needed.

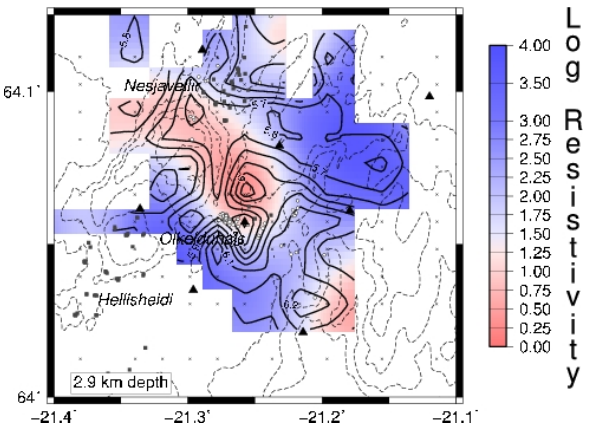

Figure 8 – Comparison between the resistivity model obtained from the inversion of TEM and magnetotelluric data (Arnasson et al., 2009) and the P-wave velocity model (continuous lines, contour interval 0.1 km/s) obtained from the tomography of broadband observations at Hengill geothermal system at 2900 m depth. Black triangles are broadband station locations.

ACKNOWLEDGEMENTS

We would like to thank Kristin Vogfjörd and Steinunn Jakobsdottir for their full support to this project and for providing the SIL data to this study. E.A. Gudnason, G. S. Hilmarsson, H. O. Stefànsson, J. E. Jonsson, S. A. Hàlldorsson, Th. Agustsdottir and Th. Björnsdottir valuably helped during the (wet) field work. We would like to hightlight a special note for Benjamin Francois for his uncounted time and help in the (musical) fieldwork. Retrieving data from some disks would not have been possible without the help of Karl-Heinz Jäckel and Luong Van-Hung. Didier Bertil and Xavier Serey helped in analysing data. Fruitful discussions with Bryndis Brandsdottir, Magnus Gudmundsson and Bernard Bourgeois are fully acknowledged. John Douglas kindly improved the English. Five broadband instruments are from the GFZ instrumental pool, and two from the BRGM instrumental pool. This study was funded by the European Community in the Sixth Framework Programme though the IGET project (contract 518378) and ENGINE project (contract 019760).

REFERENCES

Akaike, H. (1973). Information theory and an extension of the maximum likelihood principle. *In Budapest Akademiai Kiado*, pages 267-181. B. petrov and F. Csaki (Editors).

Aki K., M. Fehler and S. Das, 1977. Source mechanism of volcanic tremor: fluid-driven crack models and their application to the Kilauea eruption. *J. Volcanol. Geoth. Res*., 2, 259-287.

Allis R., 2000. Insights on the formation of vapor-dominated geothermal systems. *Proceeding WGC 2000*, Kyushu, Tohoku, Japan, 28th May-10th June, 2000.

Allis R.and Shook G.M., 1999. An alternative mechanism for the formation of The Geysers vapor-dominated reservoir. In: *Proc. 24th Workshop on Geothermal Reservoir Engineering*, Stanford University, pp. 53–63.

Almendros J, B. Chouet and P. Dawson, 2001. Spatial extent of a hydrothermal system at Kilauea Volcano, Hawaii, determined from array analyses of shallow long-period seismicity 2. Results. *J. Geophys. Res*., 106, 13581-13597, 2001.

Arnasson K., H. Eysteinsson and G. Hersir, 2009. Joint 1D inversion of TEM and MT data and 3D inversion of MT data in the Hengill area SW Iceland. *Submitted to Geothermics IGET, Special Issue.*

Arnorsson S., Gudni Alexsson and K. Saemundsson, 2208. Geothermal syetsms in Iceland. *Jökull*, 58, 269-302.

Audigane P., 2000. Caractérisation microsismique des massifs rocheux fracturés. Modélisation thermo-hydraulique. Application au concept géothermique de Soultz. *Thèse ENSG/INPL*, 217 p.

Biot M. A., 1952. Propagation of elastic waves in a cylindrical bore containing a fluid. *J. Appl. Phys*., 23, 997-1005.

Chouet, B., 1986. Dynamics of a fluid-driven crack in three dimensions by the finite difference method. *J. Geophys. Res.*, 91, 13967-13992.

Chouet B., 1996. New methods and future trends in seismological volcano monitoring. *In Monitoring and Mitigation of Volcano Hazards, Scarpa/Tilling (Ed.)*, Springer-Verlag Berlin Heidelberg, p. 23-97.

Chouet B., P. Dawson, T. Ohminato, M. Martini, G. Saccarotti, F. Giudicepietro, G. De luca, G. Milana and R. Scarpa, 2003. Source Mechanisms of explosion at Stromboli Volcano, Italy, determined by moment tensor inversions of very-long period data. *J. Geophys. Res.* , 108, 2019.

Chouet B. 2006. Modelling and understanding volcanic processes using high quality seismological data. *Géosciences*, la revue du BRGM pour une terre durable, 4, 56-63.

Dangel S., M.E. Shaepman, E.P. Stoll, R. Carniel, O. Barzandji, E.-D. Rode and J.M. Singer, 2003. Phenomenology of tremor-like signals observed over hydrocarbon reservoirs. *J. Volcanol. Geotherm. Res*., 128, 135-158.

Eberhart-Phillips, D. (1993). Local earthquake tomography: earthquake source region, pages 613-643. *Eds Iyer, H.M and Hihara K. and Chapman & Hall, London.*

Einarsson P., 2008. Plate boundaries, rifts and transforms in Iceland. *Jökull*, 58, 35-58

Evans J.,D. Eberthart-Phillips and C. H. Thurber, 1994. User's manual for SIMULPS12 for imaging vP and vP/vS: a derivative of the "thurber" tomographic inversion SIMUL3 for local earthquakes and explosions, *USGS - Open-file report*, 94-431, -101.

Evans, J. R., G. R. Foulger, B. R. Julian, and A. D. Miller (1996), Crustal Shear-Wave Splitting from Local Earthquakes in the Hengill Triple Junction, Southwest Iceland, *Geophys. Res. Lett.*, 23(5), 455–458.

Fabriol H. and A. Beauce, 1997. Temporal and spatial distribution of local seismicity in the Chipilapa-Ahuachapán geothermal area, El Salvador. *Geothermics*, 26, 5/6, 681-699.

Ferrazini V. and K. Aki, 1987. Slow waves trapped in fluid-filled infinite-crack: implication for volcanic tremor. *J. Geophys. Res*., B9, 9215-9223.

Gruszkiewicz M.S., J. Horita, J.M. Simonson, R. E. Mesmer and J.B. Hulen, 2001. Water adsorption at high temperature on core samples from The Geysers geothermal field, California, USA. *Geothermics*, 30, 2-3, 269-302.

Haberland, C., Rietbrock, A., Lange, D., Bataille, K., and Hofmann, S., 2006. Interaction between fore-arc and oceanic plate at the south-central Chilean margin as seen in local seismic data. *Geophys. Res. Lett*., 33:L23302.

Hsieh C.-H. and Ramey Jr. H.J., 1978. An inspection of experimental data on vapor pressure lowering in porous media. *Trans. Geotherm. Resourc. Counc.* 2, pp. 295–296.

Jakobsdottir S., 2008. Seismicity in Iceland, *Jökull*, 58, 75-100.

Jousset P., J. Neuberg and S. Sturton, 2003. Modelling the time-dependent frequency content of low-frequency volcanic earthquakes. J. Volcanol. Geotherm. Res., 2003, 128, 201-223.

Jousset P., J. Neuberg and A. Jolly, 2004a. Modelling low-frequency volcanic earthquakes in a viscoelastic medium with topography, *Geophys. J. Int.*, 159 (2),776-802.

Jousset P., S. Bès de Berc, H. Fabriol and B. Chouet, 2004b. Monitoring and exploration of geothermal fields using broadband seismology: application to Bouillante, Guadeloupe, *IAVCEI General Assembly, Pucon*, Chile, 14th-19th, November, Symposium 8. 508b-pf-126.

Jousset, P., 2006. Sismologie large bande: méthodologie et applications: apport en géothermie haute enthalpie à Bouillante, Guadeloupe. *BRGM Report RP-54701-FR*, page 119 pp.

Jousset P. and B. François, 2006. Set-up of a broadband seismological network at Hengill geothermal field. *BRGM report RP-54971-FR*, 51 pp.

Jousset P., C. Haberland, K. Bauer and K. Arnason, 2009. Detailed structure of the Hengill geothermal volcanic complex, Iceland, inferred from 3D tomography of high-dynamic broadband seismological data. *Submitted to Geothermics IGET, Special Issue*.

Julian B., A. Miller and G. Foulger, 1997. Non-double couple earthquake mechanisms at the Hengill-Grensdalur volcanic complex, Geophys. Res. Lett., 24, 7,743-746.

Kawakatsu H. and S. Kaneshima and T. Matsubayashi and Y. Ohminato and Y. Sudo and T. Tsutui and K. Uhira and H. Yamasato and H. Ito and D. Legrand, 2000. Aso94: Aso seismic observation with broadband instruments. *J. Volcanol. Geotherm. Res.*, 101, 129-154.

Kissling E., W. Ellworth and D. Eberhart-Phillips and U. Kradolfer, 1994. Initial reference models in local earthquake tomography. J. Geophys. Res., 99, 19635-19646.

Kumagai H. And B. Chouet, 1999. The complex frequency of long-period seismic events as probes of fluid composition beneath volcanoes. *Geophys. J. int.*, 138, F7-F12.

Kumagai H., B. Chouet and M. Nakano, 2002. Temporal evolution of a hydrothermal system in Kuratsu-Shirane volcano, Japan, infered from the complex frequencies of loing-period events, *J. Geotherm. Res.*, 107 (B10), 2236.

Legrand D., Kaneshima S. and H. Kawakatsu, 2000. Moment tensor analysis of the near field broadband waveforms observed at Aso volcano, Japan. *J. Volcanol. Geoth. Res.* 22, 59-95.

Lokmer, I., Bean, C., Saccorotti, G., and Patanè, D. (2007). Moment-tensor inversion of LP events recorded on Etna in 2004 using constraints obtained from wave simulation tests. *Geophys. Res. Lett*., 34(22):L22316.

Maeda, N. (1985). A method for reading and checking phase times in auto-processing system of seismic wave data. *Zizin=Jishin*, 38:365-379.

Miller A. and B. Julian and G. Foulger, 1998. Three-dimensional seismic structure and moment tensors of non-double couple earthquakes at the Hengill-Grensdalur volcanic complex, Iceland, *Geophys. J. Int.*, 1998, 133, 309-325.

Nakano M., H. Kumagai and B. Chouet, 2003. Source mechanism of long-period events at Kusatsu-Shirane Volcano, Japan, inferred from wave-form inversion of the effective excitation functions. *J. Volcanol. Geotherm. Res.*, 122, 149-164, 2003.

Romero A. E., J. A. Kirkpatrick, E. L. Majer and J. E. Peterson Jr., 1994. Seismic monitoring at the Geysers geothermal field. Lawrence Berkeley Laboratory, Univ. California, 10 pp.

Sigmarsson O, J. Maclennan and M. Carpentier, 2008. Geochemistry of igneous rocks in Iceland: a review. *Jökull.*, 58, 139-160.

Stefànsson, R., Bödvarsson, R., Slunga, R., Einarsson, P., Jakobsdottir, S., Bungum, H., Gregersen, S., Havskov, J., Hjelme, J., and Korhonen, H. (1993). Earthquake prediction research in the South Iceland Seismic Zone and the SIL Project. *Bull. Seismol. Soc. Am.*, 83:696-716.

Yao Z. S.and R. G. Roberts and A. Tryggvason, 1999. Calculating resolution and covariance matrices for seismic tomography with the LSQR method. *Geophys. J. Int.*, 138, 886-894.